



REGULAR ARTICLE

## Antioxidant ferulic acid prevents the aggregation of bovine $\beta$ -lactoglobulin *in vitro*

SAMPA PAL<sup>a</sup>, SANHITA MAITY<sup>a</sup>, SUBRATA SARDAR<sup>a</sup>, SHAHNAZ BEGUM<sup>a</sup>,  
RAMKRISHNA DALUI<sup>a</sup>, HASAN PARVEJ<sup>a</sup>, KAUSHIK BERA<sup>b</sup>, ANIRBAN PRADHAN<sup>c</sup>,  
NAYIM SEPAY<sup>a</sup>, SWARNALI PAUL<sup>a</sup> and UMESH CHANDRA HALDER<sup>a,\*</sup>

<sup>a</sup>Organic Chemistry Section, Department of Chemistry, Jadavpur University, Kolkata 700 032, India

<sup>b</sup>Natural Products Laboratory, Department of Chemistry, The University of Burdwan, Burdwan 713 104, India

<sup>c</sup>Director's Research Unit (DRU), Indian Association for the Cultivation of Science, Kolkata 700 032, India

E-mail: uhalder2002@yahoo.com

MS received 20 November 2019; revised 27 April 2020; accepted 4 May 2020

**Abstract.** Amyloids, a well-ordered  $\beta$ -sheet-enriched structural network, can be broadly defined as insoluble protein aggregates that are linked to a wide variety of diseases including systemic amyloidosis and some neurodegenerative disorders. Ferulic acid (FA), a phenolic acid, abundant in antioxidant and efficient pharmaceutical has beneficial effects against several ailments. Based on this, we have investigated the protective role of FA on amyloid formation of bovine  $\beta$ -lactoglobulin ( $\beta$ -lg), a model globular protein. Using a set of *in vitro* biophysical methods, such as UV-Vis spectroscopy, fluorescence, circular dichroism, transmission electron microscopy, etc., our research group has concluded that FA significantly inhibits the heat-induced amyloid formation of  $\beta$ -lg and this inhibitory effect is dose-dependent. Exposed surface hydrophobicity of  $\beta$ -lg amyloid fibrils decreased significantly in the presence of FA. Docking study revealed that ionic and hydrogen bonding interactions between FA and  $\beta$ -lg prevented protein conformational changes leading to fibrillation. We anticipate that our finding would give an insight into the protein aggregation inhibited by the antioxidant compound, FA and pave the way for finding and developing other new small molecules (protein misfolding inhibitors) that give similar result against amyloid fibril formation and its allied neurodegenerative disorders.

**Keywords.** Antioxidant; ferulic acid;  $\beta$ -lactoglobulin; aggregation.

### 1. Introduction

In the present area of research, a very interesting topic is the alteration of native (often soluble) proteins into non-native folded fibrillar structures; these are often not soluble in various solvents as well as in water. These protein fibrils are usually called amyloid fibrils and are the hallmark for numerous ailments, including Alzheimer's, Huntington's, type II diabetes, Parkinson's, prion-associated encephalopathy diseases and others.<sup>1–6</sup> Amyloid fibrils are highly organised polypeptide aggregates and are rich in  $\beta$ -sheet secondary conformation.<sup>7</sup> These fibrils are stable against temperature,<sup>8</sup> hydrolytic pressure,<sup>9</sup> proteolytic enzymes<sup>10</sup> and denaturants.<sup>11</sup> Several proteins and peptides, e.g. amyloid  $\beta$ -peptide (A $\beta$ ),  $\beta$ -lactoglobulin

( $\beta$ -lg) islet amyloid polypeptide (IAPP), insulin,  $\alpha$ -synuclein, and transthyretin have been identified as amyloidogenics,<sup>12–16</sup> but it has been observed that there is no similarity in primary structure among them.<sup>17</sup> The aggregation pattern of such peptides and proteins differs owing to their differential forms.<sup>18–20</sup>

In recent research work, a number of endeavours have been applied to find or design the compounds which can prevent the formation of these toxic oligomeric species or break up the pre-formed fibrils. Several working parameters, e.g. concentration of protein, pH of experimental solution, ionic strength of the reaction medium, reaction temperature, existence of co-solvents, etc., can be altered to modulate the aggregation process of  $\beta$ -lg into the oligomers or fibrils.<sup>21–23</sup>

Small organic molecules (either from natural origin or synthetically derived) play a significant role in

\*For correspondence

amyloid inhibition. Nanoparticles,<sup>24</sup> small molecules having antioxidative potency, e.g. vitamin C,<sup>25</sup> nicotine,<sup>26</sup> kaempferol,<sup>27</sup> and vitamin B12<sup>28</sup> have been found to reduce oxidative strain associated with neurodegenerative disorders. Curcumin, a well-known phenolic molecule, showed anti-amyloid efficacy and has been pondered for the Alzheimer's disease (AD) therapy.<sup>29</sup> Borana *et al.*, showed that curcumin prevents lysozyme fibril formation, which is not related to any neurodegenerative disorders.<sup>30</sup> A polyphenolic compound, epigallocatechin gallate has been shown to inhibit the formation of noxious amyloid of A $\beta$ <sup>31</sup> and  $\alpha$ -synuclein.<sup>32</sup> A well-established fact is that these phenolic compounds can reduce the risk of developing age-related neurodegenerative disorders, e.g. AD, Parkinson's, and Huntington diseases, and also, they prevent chronic ailments, for instance, cancers and cardiovascular diseases. Literature reports have demonstrated that they bind with proteins<sup>32,33</sup> and form complexes through weak forces, including hydrogen bonding and hydrophobic interactions. Along with the polyphenols, the phenolic acid present in the plant foods and beverages also shows anti-amyloid role against proteins/peptides linked with diseases, e.g. Alzheimer's<sup>34</sup> and diabetes mellitus.<sup>35</sup> Ferulic acid (FA), a ubiquitous phenolic acid compound, present in plants as well as in many foods has a potent antioxidant activity.<sup>36</sup> The structure of FA (4-hydroxy-3-methoxycinnamic acid), shown in Figure 1 is similar to the structure of curcumin, which directly affects the A $\beta$  peptide aggregation<sup>29,37</sup> as well as can dissociate the pre-formed A $\beta$  fibrils.<sup>38</sup> Likewise, FA has been shown to inhibit the A $\beta$  fibril formation<sup>34</sup> and destabilize the pre-formed fibrils.<sup>39</sup> Accumulating evidence showed that FA has potential therapeutic role in cancer and cardiovascular disorders as well as neurodegenerative disorders.<sup>40–43</sup>

Beta-lactoglobulin, ( $\beta$ -lg), the principal protein constituent in the whey of ruminant milk (MW 18.4 kDa), is a compactly folded small globular protein having 162 amino acid residues. In this study, our research group has chosen the bovine  $\beta$ -lg as it is extensively studied owing to its availability and high dietary importance relevant to the food industry. This

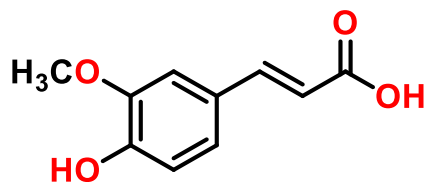


**Figure 1.** Chemical structure of *trans*-ferulic acid.

macromolecule is water soluble, consisting nine antiparallel  $\beta$ -strands and one  $\alpha$ -helix segment, in which the hydrophobic chains are mainly buried.<sup>44,45</sup> Additionally,  $\beta$ -lg has two intra-molecular disulfide linkages (Cys66-Cys160 and Cys106-Cys119) and one free -SH unit (Cys121) which is buried between the major  $\alpha$ -helix and  $\beta$ -barrel.<sup>46</sup>  $\beta$ -lg exists as a dimer at room temperature with pH ranging 5.5–7.5. However, in acidic medium (pH<3.5), it dissociates into monomeric forms due to electrostatic repulsions between the subunits. The heat-induced aggregation of  $\beta$ -lg has been widely documented, but the mechanism is not hitherto fully known.<sup>47–49</sup> Based on the experimental factors,  $\beta$ -lg forms either amorphous aggregates or amyloid fibrils.<sup>49,50</sup> In acidic medium,  $\beta$ -lg molecule can form fibrils above 75°C. Nonetheless, prolonged heating at 75°C instigates the oxidation reaction endorsing the exchange between -SH groups and S-S linkages.<sup>51</sup>

Although FA can inhibit the formation of several amyloid fibrils, the inhibitory action of FA against  $\beta$ -lg has not hitherto been accounted. In this present study, we investigated the inhibitory effects of FA on heat-induced fibril formation of  $\beta$ -lg *in vitro*. We studied the influence of FA on the morphology of  $\beta$ -lg fibril by using transmission electron microscopy (TEM). The inhibition of  $\beta$ -lg amyloid fibril formation has been confirmed by Congo red (CR) and Thioflavin T (ThT) binding studies, utilizing UV-Vis and fluorescence spectroscopy. The secondary conformational changes during fibril formation and its inhibition upon addition of FA have been directly monitored by CD and FTIR spectroscopic measurements. Moreover, the outcomes of molecular docking study showed the considerable mode of interaction and sites of interaction between  $\beta$ -lg and FA.

## 2. Experimental

### 2.1 Reagents and chemicals

Isolation and purification of bovine  $\beta$ -lg from cow's milk was performed as previously described.<sup>52</sup> Total purified material was lyophilized and kept at 4°C for further use. As the extinction coefficient of  $\beta$ -lg (0.959 mg<sup>-1</sup> mL<sup>-1</sup> cm<sup>-1</sup> at 280 nm) is known, different concentrations of  $\beta$ -lg solutions were made by dissolving lyophilized protein in Milli-Q water and checking the absorbance at 280 nm. Sodium dihydrogen phosphate (NaH<sub>2</sub>PO<sub>4</sub>), *trans*-ferulic acid (FA, 128708) were obtained from Sigma Aldrich (USA), and different fluorescent probes, namely 8-anilino-naphthalene-1-sulfonic acid ammonium salt (ANS), Congo red (CR) and Thioflavin T (ThT) were purchased

from Sigma Chemical (St. Louis, USA) and utilized as such. All the other reagents utilized in our experiments were of analytical grade or high purity reagent available.

## 2.2 Protein sample preparation

Stock solution of  $\beta$ -Ig, used in each experiment was made in  $\text{NaH}_2\text{PO}_4$  buffer (10 mM) at pH 7.4 to get a final  $\beta$ -Ig concentration of 3 mM. Stock solution of FA, because of its poor aqueous solubility was prepared freshly by first dissolving it in ethanol and then diluting with  $\text{NaH}_2\text{PO}_4$  buffer in order to get the final FA concentration in solution of 3 mM. Appropriate volumes of  $\beta$ -Ig, FA stock solutions and 10 mM buffer were mixed to get 1:0, 1:1, 1:3, 1:4, 1:5 and 1:10 molar ratio of  $\beta$ -Ig:FA.  $\beta$ -Lg fibril formation was monitored by heating these  $\beta$ -Ig-FA mixtures at 75°C over a period of 1 h prior to all experiments. The required  $\beta$ -Ig concentrations were attuned for all the experiments.

## 2.3 Intrinsic fluorescence study

Intrinsic fluorescence was measured by using a Shimadzu spectrofluorometer (Shimadzu 5301 PC) at an excitation wavelength of ( $\lambda_{\text{ex}}$ ) 295 nm. The spectral resolution for both excitation and emission was set at 5 nm. Fluorescence experiments were conducted with all protein solutions as depicted above in 10 mM buffer, pH 7.4 and at 25°C.  $\beta$ -Ig (concentration 13.6  $\mu\text{M}$ ) intrinsic fluorescence emission were measured by using a quartz cell with a path length of 1 cm in the wavelength ranging from 300 to 400 nm, and all measurements were done in triplicate.

## 2.4 1-Anilinonaphthalene-8-sulfonate (ANS) fluorescence study

Surface hydrophobicity of  $\beta$ -Ig fibrils in the absence and presence of FA was determined by 1-anilinonaphthalene-8-sulfonate (ANS), a polarity-sensitive fluorescent probe.<sup>53</sup> For this, a stock solution of ANS was added to each aliquot of  $\beta$ -Ig solution to get a final ANS concentration of 30  $\mu\text{M}$ . Typically, ANS concentration was 50 molar excess of protein concentration. The ANS-fluorescence emissions (400–650 nm) were measured using Shimadzu RF-5301 PC with excitation at 380 nm. Slit widths were set at 5 nm for both excitation and emission. Each spectrum was blank corrected. The data reported were means of three replicates.

## 2.5 Thioflavin T (ThT) fluorescence assay

Thioflavin T, a dye bound to amyloid fibrils, shows enhanced fluorescence emission at 480 nm.<sup>54</sup> To explore and compare the fibrils formed by protein ( $\beta$ -Ig) in the absence and presence of FA, the following assay was

employed using ThT as a probe. Concisely, 250  $\mu\text{L}$  of sample solutions (1 mg  $\text{mL}^{-1}$ ) were added separately to 20  $\mu\text{L}$  ThT solution (stock 3.13 mM ThT in buffer (10 mM), pH 7.4) containing 1.73 mL of buffer (pH 7.4, 10 mM), mixed and incubated for 30 min. The final ThT and protein concentration were 30  $\mu\text{M}$  and 6.8  $\mu\text{M}$ , respectively. After 30 min of incubation with ThT dye, the ThT fluorescence of working solutions were studied by a Shimadzu spectrofluorometer (Shimadzu 5301 PC) with an excitation wavelength of 450 nm<sup>22</sup> and emission recorded from 460 nm to 650 nm. Excitation and emission slit widths were same (5 nm). All solutions were measured at least thrice, and the data taken were averaged. All measurements were done at 25°C.

## 2.6 Rayleigh light scattering (RLS) study

The heat-induced  $\beta$ -Ig aggregation in the absence and presence of FA was quantified by RLS experiments. After exciting the working solutions at 350 nm, mentioned in figure caption 3B, the fluorescence intensities were recorded at 350 nm in a Shimadzu spectrofluorometer (Shimadzu 5301 PC). All sample solutions were prepared in  $\text{NaH}_2\text{PO}_4$  buffer (10 mM) at pH 7.4, and we used a quartz cell and 1 cm path length for measurements. Emission and excitation slits were 5 nm. These experiments were performed in triplicate.

## 2.7 Congo red (CR) assay

To evaluate the influence of FA on formation of heat-induced  $\beta$ -Ig aggregates, CR assay was applied. The CR absorption spectra were recorded from 400 to 600 nm. Samples for aggregation experiments were prepared as follows. For this, 60  $\mu\text{L}$  heated working solutions (5 mg  $\text{mL}^{-1}$ ) was mixed with 500  $\mu\text{L}$  of CR solution (100  $\mu\text{M}$ ) in buffer (10 mM, pH 7.4). Requisite volume of buffer solution was added to get a total volume of 2 mL for each solution.<sup>55</sup> Concentrations of CR and protein were 25  $\mu\text{M}$  and 8.2  $\mu\text{M}$ , respectively.

## 2.8 Circular dichroism (CD) spectroscopy

Far-UV CD spectra of heat-treated  $\beta$ -Ig in the presence and absence of different concentrations of FA in 10-mM phosphate buffer (pH 7.4) were completed using Jasco Spectropolarimeter (J-815) with a quartz cell (path length=1 nm) at 20°C.  $\beta$ -Ig concentrations (0.25 mg  $\text{mL}^{-1}$ ) were kept constant for far-UV CD measurements. A far-UV CD spectrum was also recorded for a 0.25 mg  $\text{mL}^{-1}$  native protein solution in the same phosphate buffer. All data reported here was average of three sequential experiments. Averaged scans of solvent spectrum were subtracted from protein ( $\beta$ -Ig) scans to obtain the final spectrum. The far

UV-CD spectra were fixed into a curve-fitting program CDNN 2.1 to ascertain the percent (%) of secondary structures present in  $\beta$ -lg under different experimental conditions.

### 2.9 Dynamic light scattering (DLS) measurements

The diffusion of small particles in solution induces fluctuations in the intensity of the scattered light. DLS detects these fluctuations using an autocorrelator on a microsecond time scale and is used to analyze the distribution of molecules and supramolecular aggregates as it is very sensitive to particle size.<sup>56</sup> DLS measurements were conducted with heated  $\beta$ -lg solutions in the absence and presence of different concentration of FA using Zetasizer Nano (Malvern Instrument, UK). The sample solutions were illuminated by a 633-nm laser. A rectangular 2-mL cuvette was used for holding samples having 10 mm path length. All experiments were performed at 20°C, taking 2 mL solutions (0.25 mL of sample and 1.75 mL buffer). The time-dependent autocorrelation function was obtained with 12 acquisitions for every run. The data reported were means of five experiments.

### 2.10 Fourier transform infrared (FTIR) spectroscopy

FTIR spectra were collected by utilizing a Spectrum 100 FT-IR spectrometer (Perkin-Elmer) at a nominal resolution of  $2\text{ cm}^{-1}$  in  $\text{N}_2$  atmosphere. For FTIR experiments, 50  $\mu\text{L}$  native and heattreated  $\beta$ -lg solutions (in the absence and presence of the FA)  $20\text{ mg mL}^{-1}$  were taken in a Microcon filter device and diluted with  $\text{D}_2\text{O}$  (200  $\mu\text{L}$ ). Then, the solution was immediately centrifuged ( $4000\times g$ , 10 min) until the volume reached up to 50  $\mu\text{L}$ . Another 200  $\mu\text{L}$  of  $\text{D}_2\text{O}$  was added and centrifuged. This  $\text{D}_2\text{O}$  exchange process was repeated thrice. Finally, the  $\text{D}_2\text{O}$  exchanged protein solutions were taken for FTIR scans ( $1550\text{--}1750\text{ cm}^{-1}$ ). Spectrum of  $\text{D}_2\text{O}$  background at pH 7.0 was taken and subtracted from the raw sample spectrum. The band positions were then assigned according to the standard protocol.<sup>57</sup>

### 2.11 High resolution transmission electron microscopy (HRTEM)

A HRTEM (JEOL-HRTEM-2011, Tokyo, Japan) with an accelerating voltage of 80–85 kV in different magnifications was applied using 5  $\mu\text{L}$  of sample solutions to observe the images of  $\beta$ -lg aggregates ( $\beta$ -lg concentration 10  $\mu\text{M}$ ). Prior to HRTEM assay, all heat-treated sample solutions were sonicated for 1 h and diluted 50–150 times with buffer (pH 7.4). Two drops of each diluted sample were spotted onto a carbon-coated copper grid (300 C mesh,

ProSciTech). After 20 s, excess sample was soaked away from the grid using filter paper and subsequently, a drop of 2% uranyl acetate (Sigma, Steinheim, Germany) in  $\text{H}_2\text{O}$  was added for 15 min. Excess reagent was removed, left for air drying and air-dried specimens were utilized for imaging study. All samples were left to equilibrate for 6 h before getting the image.

### 2.12 Molecular docking study

The AutoDock 4.2.0 based docking studies of FA molecule with  $\beta$ -lg (2BSY) were carried out. The structure of FA used in docking after minimized its energy by DFT optimization using Gaussian 09W. Lamarckian genetic algorithm (LGA) was utilized for molecular docking. In this calculation,  $126 \times 126 \times 126$  grid box was used.

## 3. Results and Discussion

### 3.1 Microenvironment change of $\beta$ -lg investigated by intrinsic fluorescence

To study the effect of FA on the heat-induced conformational alteration of  $\beta$ -lg, intrinsic fluorescence spectral measurements were performed. The inhibitory effect of FA was examined at five different molar ratios of FA, as stated in the caption of Figure 2A. Native  $\beta$ -lg has two tryptophan moieties and the intrinsic fluorescence property of  $\beta$ -lg is almost exclusively due to the tryptophan 19 (Trp 19) residue.<sup>58</sup> It exhibits the characteristic fluorescence emission maximum at 334 nm by fixing the excitation wavelength at 295 nm. As evident from Figure 2A (profile b), in the absence of FA, heated  $\beta$ -lg exhibited a distinct fluorescence spectrum as native  $\beta$ -lg. The red shift of the tryptophan fluorescence spectrum of heat-exposed  $\beta$ -lg reflected significant enhancement of the accessibility of tryptophan moiety (Trp 19) of protein to the solvent. Figure 2A (profiles c–g) showed the fluorescence intensity of  $\beta$ -lg decreased regularly with gradual addition of FA into a fixed concentration of  $\beta$ -lg solutions. This suggested a concentration-dependent change in the intrinsic fluorescence of the heat-exposed  $\beta$ -lg in presence of FA (Figure 2A). Additionally, much lower fluorescence intensities were found in  $\beta$ -lg:FA (1:5 and 1:10) systems (profiles f&g of Figure 2A) than other ratios of  $\beta$ -lg:FA systems. The decrease in fluorescence intensities, in fact, may be due to the change in polarity of microenvironments around the tryptophan moieties in presence of FA. At 1:10 molar ratio of  $\beta$ -lg to FA, the highest inhibitory effect of FA was noticed from the lowest fluorescence intensity of the solution, shown in profile g

(Figure 2A). Thus, FA showed inhibitory effect on temperature-induced amyloid formation of  $\beta$ -Ig.

At this point, the protein-structure deformation effect of ethanol, which comes from the ethanolic solution of FA needs to be discussed here. In these experiments, the stock solutions of FA and the protein are 10 mM and 183  $\mu$ M, respectively. Overall, to prepare 2 mL  $\beta$ -Ig (45  $\mu$ M) and FA solution of 1:10 ratio, the required ethanol is 4.5% ethanolic solution. Previous studies showed that the ethanol has the ability to form aggregates of  $\beta$ -Ig under similar heating conditions at 30% and above ethanol concentrations.<sup>59a-c</sup> Thus, the organic solvent ethanol accelerates only the aggregation of  $\beta$ -Ig at higher concentrations. In our cases, the concentration of ethanol used was sufficiently low. Hence, it is clear that no  $\beta$ -Ig aggregation or disaggregation effect was possible with this low ethanol concentration.

### 3.2 ANS-fluorescence study to observe the hydrophobicity change of $\beta$ -Ig

The change of hydrophobicity of  $\beta$ -Ig during thermal aggregation in the absence and presence of FA was monitored by collecting the ANS emission spectra. Evidently, ANS, a fluorescent hydrophobic probe, binds to molten globule state of proteins and shows fluorescence intensity.<sup>60</sup> The interaction of ANS with  $\beta$ -Ig may be due to both electrostatic and hydrophobic interactions.<sup>61</sup> Figure 2B shows the ANS fluorescence spectra of heat-treated  $\beta$ -Ig in sodium phosphate buffer (pH 7.4). Generally, heat-induced  $\beta$ -Ig showed ANS fluorescence signal at around 480 nm at pH 7.4 (profile

b, Figure 2B) with a greater ANS intensity than native  $\beta$ -Ig (profile a, Figure 2B). This rise of fluorescence intensity may be ascribed to further entrance of ANS to hydrophobic loops present in thermally exposed  $\beta$ -Ig compared to native  $\beta$ -Ig. Thus, increase in hydrophobic loops enhances the protein-protein interactions leading to more thermal aggregation of  $\beta$ -Ig.<sup>62</sup> However, we obtained significant different results when  $\beta$ -Ig was incubated (75°C, 1 h) in the presence of different FA concentrations, mentioned in figure caption (profiles c–g, Figure 2B). The  $\beta$ -Ig fluorescence intensity was found to be decreased considerably, indicating less disclosure of hydrophobic loops of  $\beta$ -Ig, and thus, FA efficiently inhibited the amyloid fibril formation of  $\beta$ -Ig. Further, the lowest fluorescence intensity of  $\beta$ -Ig-FA solution was observed at much higher concentrations of FA (10-fold molar excess) (profile g, Figure 2B), demonstrating a minimum binding of ANS. This was strongly supported by our ThT data given below.

### 3.3 Formation of aggregates monitored by ThT assay

To determine the inhibitory activity of FA on temperature-induced  $\beta$ -Ig amyloid fibrillation, we used Thioflavin T (ThT) dye which is a non-covalent reporter of amyloid aggregates and often utilized to report the aggregation behavior of proteins. Usually, ThT binds to amyloid aggregates and as a consequence, the dye shows enhanced fluorescence emission significantly.<sup>63</sup> Formation of a hydrogen bond between ThT and amyloid fibrils is reported to play a

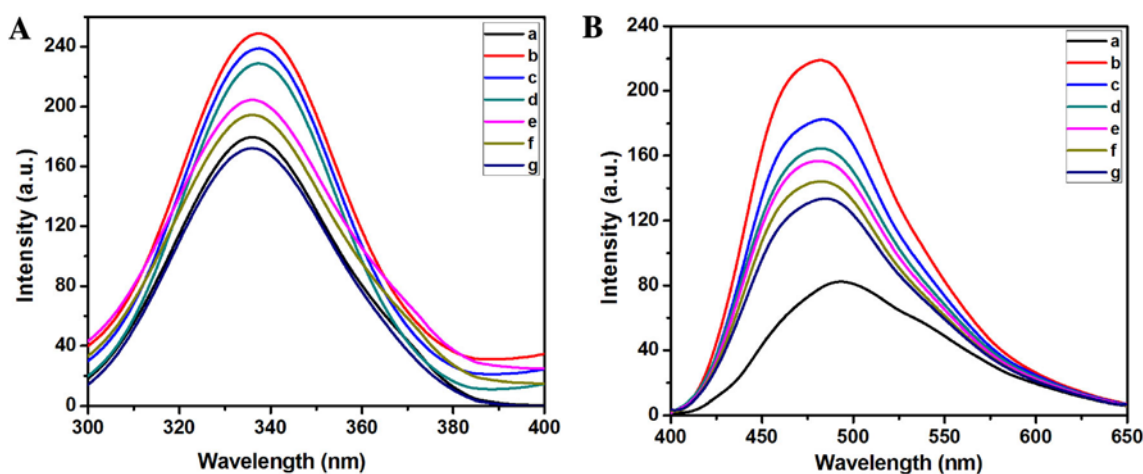


**Figure 2.** (A) Intrinsic tryptophan fluorescence and (B) ANS fluorescence emission spectra of (a) native  $\beta$ -Ig, heat exposed (75°C), (b)  $\beta$ -Ig, (c)  $\beta$ -Ig:FA (1:1), (d)  $\beta$ -Ig:FA (1:3), (e)  $\beta$ -Ig:FA (1:4), (f)  $\beta$ -Ig:FA (1:5) and (g)  $\beta$ -Ig:FA (1:10).  $\beta$ -Ig concentrations throughout all emission experiments were kept at 0.25 mg mL<sup>-1</sup>. Results were the mean of three different experiments.

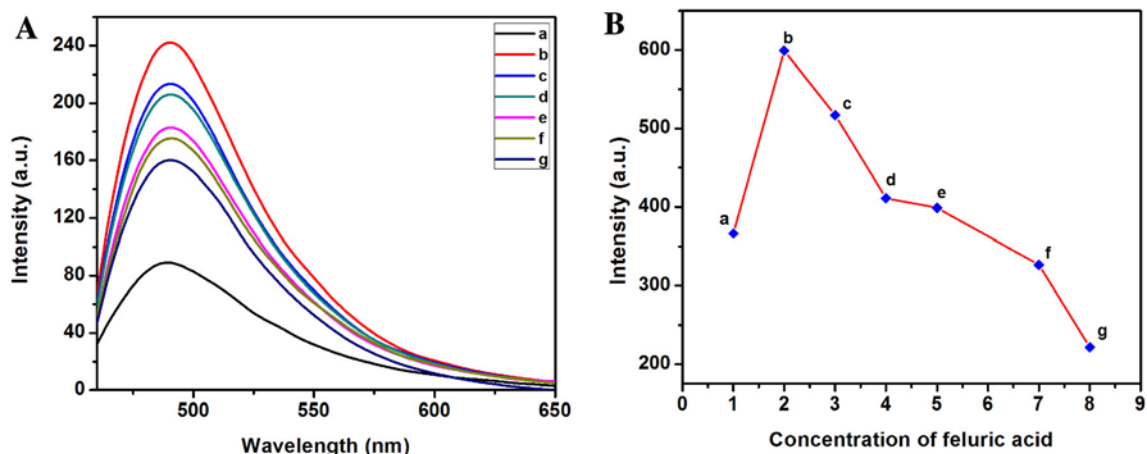


**Figure 3.** (A) ThT fluorescence spectral changes of heated (75°C for 1 h)  $\beta$ -Ig in the absence and presence of FA. Line (a) native  $\beta$ -Ig, line (b) heat treated  $\beta$ -Ig, lines (c–g) correspond to heated  $\beta$ -Ig in presence of FA: (c)  $\beta$ -Ig:FA (1:1), (d)  $\beta$ -Ig:FA (1:3), (e)  $\beta$ -Ig:FA (1:4), (f)  $\beta$ -Ig:FA (1:5), and (g)  $\beta$ -Ig:FA (1:10).  $\beta$ -Ig concentrations were  $0.25 \text{ mg mL}^{-1}$ . (B) Effect of increasing concentration of FA on the fibrillation of  $\beta$ -Ig heated at 75°C in  $\text{NaH}_2\text{PO}_4$  buffer (pH 7.4, 10 mM) as monitored by RLS measurement.  $\beta$ -Ig concentration was  $0.25 \text{ mg mL}^{-1}$ . Points a–g: (a) native  $\beta$ -Ig, heat treated: (b)  $\beta$ -Ig:FA (1:0), (c)  $\beta$ -Ig:FA (1:1) (d)  $\beta$ -Ig:FA (1:3), (e)  $\beta$ -Ig:FA (1:4), (f)  $\beta$ -Ig:FA (1:5), and (g)  $\beta$ -Ig:FA (1:10). Results were the mean of three different experiments.

role in the enhancement of ThT fluorescence intensity at maximum wavelength (490 nm).<sup>64</sup> Figure 3A displays the ThT fluorescence intensities of different  $\beta$ -Ig samples. We have observed a strong increase in ThT emission intensity of heated  $\beta$ -Ig at 490 nm (Figure 3A, curve b), typical alter for amyloid fibrils. Even though the interaction between ThT and amyloid fibrils is not yet known clearly, the literature reports<sup>65,66</sup> suggest that this interaction depends on the amyloidogenic protein along with binding pattern.<sup>67</sup> Nonetheless, enhanced fluorescence intensity at 490 nm confirms the formation of  $\beta$ -Ig amyloid fibrils. ThT intensity of  $\beta$ -Ig decreased regularly with the variation of FA concentration (Figure 3A, curves c–g), suggesting the efficient concentration-dependent inhibitory effect of FA on the fibril formation of  $\beta$ -Ig. In  $\beta$ -Ig–FA mixture with 1:10 molar ratio, the ThT showed lowest fluorescence emission intensity and this indicated that the maximum inhibitory effect of FA on  $\beta$ -Ig fibrillation appeared at 10 times excess concentrations. Thus, FA played a significant role in the protective effect of  $\beta$ -Ig fibrillation. This result also corroborated with TEM imaging of different  $\beta$ -Ig fibrils.

#### 3.4 Rayleigh light scattering (RLS) detected $\beta$ -Ig aggregates

RLS is commonly utilized to detect aggregation of proteins.<sup>68</sup> The result in Figure 3B showed the RLS

data of heat-induced  $\beta$ -Ig aggregates in the absence and presence of FA. Usually on thermal denaturation, the structure of a protein is lost and it forms aggregates. An increase in scattering intensity was observed in thermally exposed  $\beta$ -Ig (point b) than native  $\beta$ -Ig (point a), signifying the formation of  $\beta$ -Ig aggregates. Additionally, points c–g showed the RLS intensities of  $\beta$ -Ig in the presence of different molar ratios of FA. In these points, the fluorescence intensity decreased gradually with increasing FA concentration. Lowest scattering intensity of the solution (one-third) was observed when  $\beta$ -Ig to FA molar ratio reached 1:10, indicating the maximum inhibition of aggregation as evidenced by ThT analysis (point g, Figure 3B). Hence lowering RLS intensities of the incubated  $\beta$ -Ig–FA samples corroborated the thermal disaggregation of  $\beta$ -Ig by FA.

#### 3.5 CR assay

The amyloid fibril aggregates present in solutions can also be detected by CR binding analysis. CR, a secondary diazo dye interacts with  $\beta$ -sheet structures<sup>21</sup> and exhibits a bathochromic shift in the absorbance maximum (480–490 nm). The heated  $\beta$ -Ig without FA at pH 7.4 showed absorbance maximum at 490 nm (Figure 4A, profile b). This shift in the absorbance maximum of heated  $\beta$ -Ig without FA might have occurred due to the formation of amyloid-like aggregates. The addition of FA to  $\beta$ -Ig significantly affected

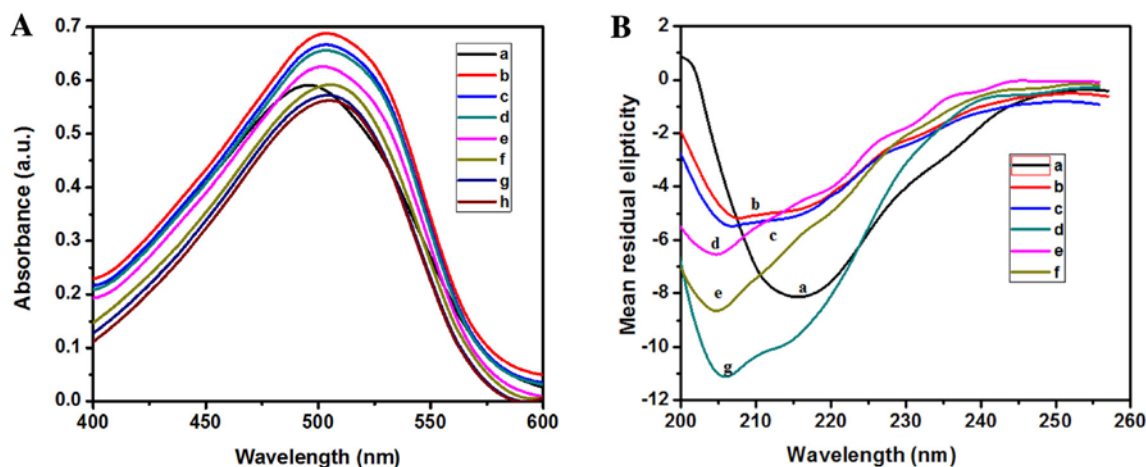


**Figure 4.** (A) CR absorption spectral alteration demonstrating the inhibition of thermal (75°C, 1 h) aggregation of  $\beta$ -lg by FA. Line (a) native  $\beta$ -lg, lines (b–g) correspond to heated  $\beta$ -lg in the presence of different concentration of FA, (b)  $\beta$ -lg:FA (1:0), (c)  $\beta$ -lg:FA (1:1), (d)  $\beta$ -lg:FA (1:2), (e)  $\beta$ -lg:FA (1:3), (f)  $\beta$ -lg:FA (1:4) (g)  $\beta$ -lg:FA (1:5) and (h)  $\beta$ -lg:FA (1:10). Final concentrations of  $\beta$ -lg in solutions were  $0.5 \text{ mg mL}^{-1}$ . (B) Far-UV CD spectra (200–260 nm) of (a) native  $\beta$ -lg, heated (75°C, 1 h), (b)  $\beta$ -lg along, (c)  $\beta$ -lg:FA (1:1), (d)  $\beta$ -lg:FA (1:3), (e)  $\beta$ -lg:FA (1:5) and (f)  $\beta$ -lg:FA (1:10) showing secondary structural changes in thermal fibrillation of protein.

the thermal aggregation profile of the protein in a dose-dependent way, and a decrease in absorption intensity was noticed (Figure 4A, profiles c–h). The decrease in absorption intensity of incubated  $\beta$ -lg samples measured in the presence of FA indicated that FA inhibited the formation of  $\beta$ -sheet structures. Adding a high molar excess of FA (1:10 molar ratio of  $\beta$ -lg to FA) resulted in the lowest absorbance for  $\beta$ -lg-FA mixture (profile g, Figure 4A), indicating the maximum inhibitory effect of FA at this particular molar ratio. Thus, at 1:10 molar ratio of  $\beta$ -lg to FA, FA stabilized more for the monomeric and dimeric structures of  $\beta$ -lg, and thus, can significantly suppress the formation of fibrillar aggregates. This result supported the ThT fluorescence measurements.

### 3.6 Changes in secondary structure of $\beta$ -lg in the presence of FA

Far-UV CD technique was employed to investigate the potential effect of FA on the secondary structural transformation of  $\beta$ -lg.  $\beta$ -lg was incubated with or without FA for 1 h (75°C) and the presence of  $\beta$ -sheet was determined by CD spectroscopy. Generally, CD spectra provided the typical information about  $\beta$ -sheet structure linked with amyloid fibril. CD spectra of incubated solutions were carried out by scanning the spectra in the spectral region of 200–260 nm at different concentrations of FA. CD spectra of  $\beta$ -lg in the presence and absence of FA is represented in Figure 4B. CD spectra of native  $\beta$ -lg (profile a,

Figure 4B) showed two negative bands at 207 and 216 nm. These two bands of  $\beta$ -lg represented the existence of ordered secondary structural content that contained  $\alpha$ -helix and  $\beta$ -sheet.<sup>69</sup> After heating at 75°C, the CD spectrum of  $\beta$ -lg showed a significant shift of the band position (profile b, Figure 4B). The heated  $\beta$ -lg showed a decrease in  $\alpha$ -helix content and an increase in the  $\beta$ -sheet (Table 1). We have also analyzed the change of secondary structure of heated  $\beta$ -lg with FA at different molar concentrations (profiles c–g, Figure 4B). It has been shown that at 1:1 molar ratio of  $\beta$ -lg:FA, a very small change of peak position with negative ellipticity value differing from heated  $\beta$ -lg was observed. CD spectra of  $\beta$ -lg:FA (1:3) showed lower MRE values at 215 and 207 nm (profile d, Figure 4B). It is of importance that the shape of the CD spectra for  $\beta$ -lg at higher ratios of FA (1:5 and 1:10, molar ratio) showed more negative MRE values with the bands between 206 and 207 nm, respectively and the disappearance of band near 215 nm, indicating the structural transitions leading to the disaggregation of fibrillar structure. The difference in MRE values could be related to the different concentrations of FA, an inhibitor of protein aggregation. One interesting observation was the maximum inhibitory effect of FA at 1:10 molar ratio on the thermal fibrillation of  $\beta$ -lg. The calculated results obtained from CD (Table 1) also revealed that the secondary structure of  $\beta$ -lg was strongly affected by the addition of FA. Our result thus support that ferulic acid (FA), a natural oxidant, can inhibit the fibrillation of  $\beta$ -lg in a concentration-dependent way.

**Table 1.** Percentage of  $\alpha$ -helix,  $\beta$ -sheet,  $\beta$ -turn and random coil of native  $\beta$ -lg, heated  $\beta$ -lg with or without FA as determined by CD calculations.

Sample	$\alpha$ -Helix (%)	$\beta$ -Sheet (%)	$\beta$ -Turn (%)	Random coil (%)
Native $\beta$ -lg	11.6	38.43	12.46	37.51
Heated $\beta$ -lg	10.67	41.33	12.24	35.76
Heated $\beta$ -lg:FA (1:1)	10.77	40.22	11.59	37.42
Heated $\beta$ -lg:FA (1:3)	11.98	39.67	12.80	35.55
Heated $\beta$ -lg:FA (1:5)	11.69	39.14	12.52	36.65
Heated $\beta$ -lg:FA (1:10)	11.56	38.16	12.84	37.34

### 3.7 Dynamic light scattering (DLS) revealed the size of $\beta$ -lg aggregates

To corroborate our above-mentioned result, we employed DLS experiments. The  $\beta$ -lg aggregates were analyzed through DLS experiments to analyze the effects of various FA ratios on the average hydrodynamic radii of  $\beta$ -lg aggregates. Scattered light intensity versus size in radius of different protein solutions was displayed in Figure 5A. Curve 'a' in Figure 5A showed the size distribution of native  $\beta$ -lg. The size distribution curves (Figure 5A, b–f) of heated (75°C)  $\beta$ -lg with and without FA (1–10 molar ratios) showed the formation of different size aggregates of protein. DLS result showed a greater light scattering intensity of heated  $\beta$ -lg (Figure 5A, curve b) as a result of greater particle size.<sup>70</sup> With the addition of FA, the scattering intensity of  $\beta$ -lg solution decreased. At  $\beta$ -lg:FA = 1:1 molar ratio, the size of the aggregates decreased minimally in the range of 30–350 nm and small-size diameter became prominent (Figure 5A,

curve c). Further increase in the molar concentration of FA showed the size of the aggregates decreased gradually (Figure 5A, curves d–f). From this analysis, we again showed that at 1:5 and 1:10 molar concentration ratio of  $\beta$ -lg:FA, FA strongly suppressed the fibrillation of  $\beta$ -lg and the size of aggregates decreased largely in the Figure 5A, curve e and f respectively. Thus, on heating  $\beta$ -lg with FA at 75°C, large size  $\beta$ -lg particles (aggregates) decreased and the light scattering was controlled by FA with smaller diameter. Therefore, according to the results, it can be concluded that FA inhibited the formation of fibrillar aggregates of  $\beta$ -lg.

### 3.8 Secondary structural composition revealed by ATR-FTIR analysis

IR technique is commonly employed to understand the secondary structural composition of protein. Thus, this technique was employed to confirm the  $\beta$ -sheet

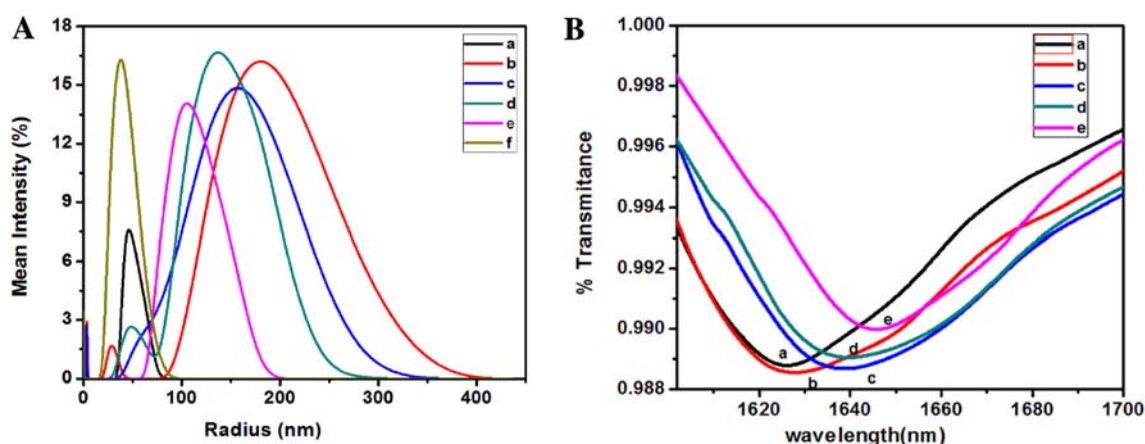


**Figure 5.** (A) A plot of mean intensity versus radius of aggregates of native  $\beta$ -lg (curve a),  $\beta$ -lg:FA (1:0) (curve b),  $\beta$ -lg:FA (1:1) (curve c),  $\beta$ -lg:FA (1:3) (curve d),  $\beta$ -lg:FA (1:5) (curve e) and  $\beta$ -lg:FA (1:10) (curve f). Samples (curve b–f) were treated at 75°C in 10 mM sodium phosphate buffer (pH 7.4, 1 h) and concentration of  $\beta$ -lg was kept at 54.35 mM. Every spectrum is mean of 48 scans. (B) FT-IR spectra of amide-I region of  $\beta$ -lg:FA mixture at different molar ratios [native (a), heated: (b) 1:0, (c) 1:1 (d) 1:5 and (e) 1:10]. Sample solutions were incubated in buffer at 75°C. Concentrations of  $\beta$ -lg were 20 mg mL<sup>-1</sup>. Reported every spectrum was a mean of 32 scans in D<sub>2</sub>O measured at 25°C.

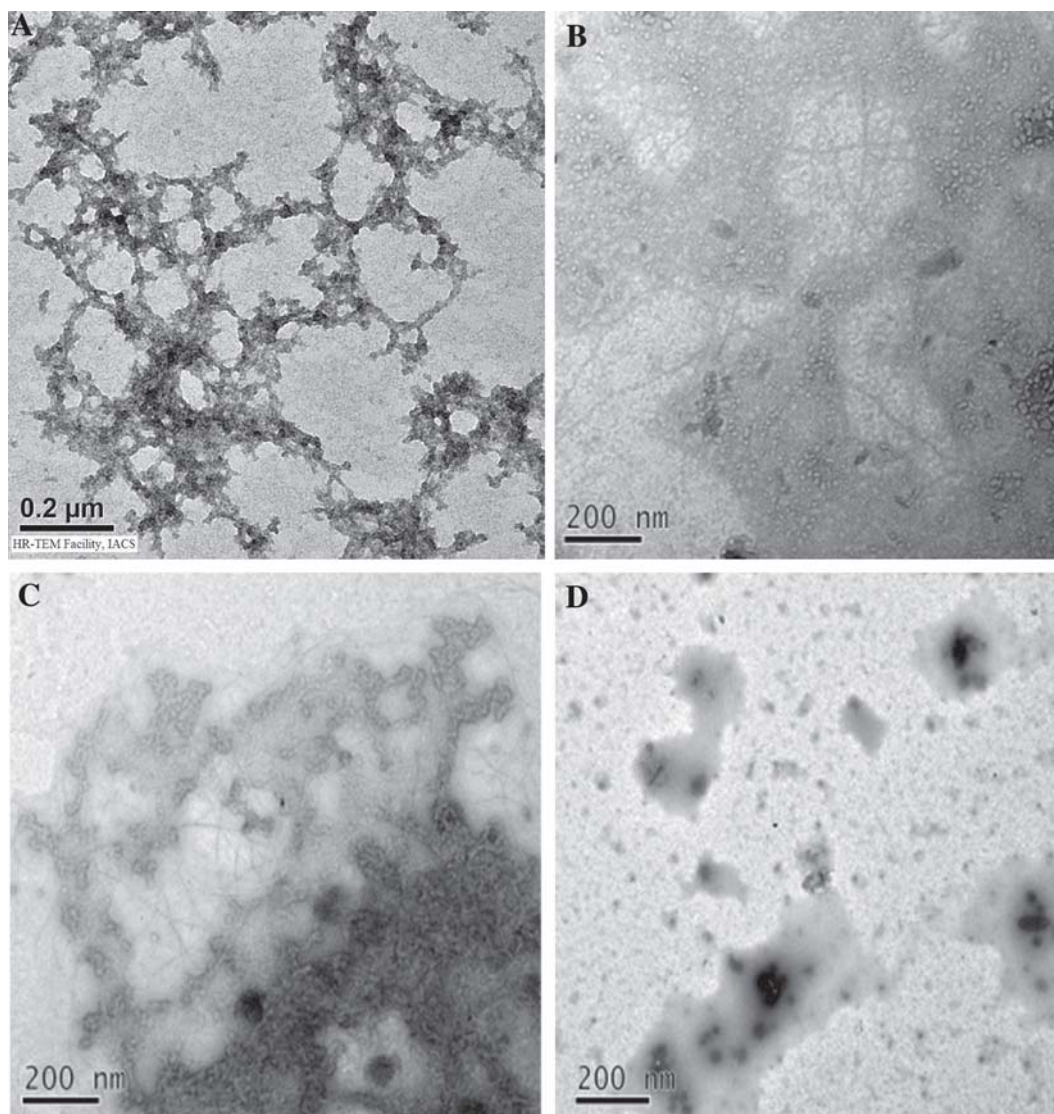


**Figure 6.** Selected TEM images of  $\beta$ -lg fibrils. (A) Heat-treated  $\beta$ -lg, (B) heat-treated  $\beta$ -lg:FA (1:1), (C) heat-treated  $\beta$ -lg:FA (1:5), and (D) heat-treated  $\beta$ -lg:FA (1:10). All samples were heated at 75°C for 1 h.

structure formation during fibrillation of  $\beta$ -lg (75°C) in the presence of FA. The secondary structure of  $\beta$ -lg can be acquired on the basis of infrared assignment of the amide-I band ranging from 1600 to 1700  $\text{cm}^{-1}$  of ATR-FTIR spectra. The amide-I band of native  $\beta$ -lg molecule appears at around 1629  $\text{cm}^{-1}$  (Figure 5B, profile a) which is the typical feature for the protein like  $\beta$ -lg having predominant  $\beta$ -sheet structure.<sup>62</sup> In the absence of FA, the IR spectrum of heated  $\beta$ -lg exhibited a band roughly at 1633  $\text{cm}^{-1}$  (profile b) that indicated an increase in  $\beta$ -sheet structure in comparison to native  $\beta$ -lg owing to self-assembly of the protein. In presence of FA at 1:1 molar ratio with  $\beta$ -lg, FTIR showed a peak centered at 1642  $\text{cm}^{-1}$  (profile c) which indicated deformation or structural transition of  $\beta$ -sheet structure. At  $\beta$ -lg to FA molar ratio of 1:5 and 1:10, the peak positions were shifted between 1640

$\text{cm}^{-1}$  and 1646  $\text{cm}^{-1}$ , respectively (profiles d and e). Thus, the increased concentration of FA shifted the peak positions due to the structural transitions towards random coil structure. Therefore, it may be concluded that FA at higher concentration strongly inhibited the heat-induced fibrillation of  $\beta$ -lg. This IR results were in harmony with the conclusion obtained from our CD experiment.

### 3.9 TEM results distinguished the morphology of $\beta$ -lg aggregates with FA

The HR-TEM study was also performed to ascertain whether FA affected the heat-induced aggregation and fibril formation of  $\beta$ -lg (Figure 6). The heat-exposed  $\beta$ -lg without FA formed the self-assembly (Figure 6A)

**Table 2.** Comparison of the classes of compounds showing protein aggregation inhibitory activity.

Entry	Compounds (C)	Protein (P)	Mole ratio (P:C)	References
1	Curcumin	$\beta$ -Ig	1:1	71
2	Curcumin	A $\beta$	1:8	72
3	FA	A $\beta$	1:4	73
4	FA	$\beta$ -Ig	1:10	Present study
5	Phenol red	A $\beta$	1:9.6	
6	Indomethacin	A $\beta$	1:21	72
7	Quinacrine mustard dihydrochloride	A $\beta$	1:46	72
8	Pherphenazine	A $\beta$	1:56	72
9	Eosin Y	A $\beta$	1.62	72

and the morphology was totally fibrillar. However, the TEM image of  $\beta$ -Ig in the presence of FA showed that the aggregation was reversed to a different extent. When the  $\beta$ -Ig:FA molar ratio was 1:1, no significant morphological change of fibrillar structure was observed and only intensity of aggregation was reduced (Figure 6B), but when the amount of FA was increased, the fibrillation of  $\beta$ -Ig decreased. The amyloid fibrillation decreased significantly when the  $\beta$ -Ig:FA molar ratios were 1:5 and 1:10 respectively (Figure 6, C&D). These findings clearly suggest that at 1:5 and 1:10  $\beta$ -Ig:FA molar ratios, FA showed strong protective effect on  $\beta$ -Ig aggregation. Therefore, our *in vitro* observations demonstrate that FA has potent anti-fibrillogenic activity on bovine  $\beta$ -Ig aggregation.

### 3.10 Competitive protein aggregation inhibitory effect of FA

To check the potency of FA as a protein aggregation inhibitor, we compared it with other reported compounds' inhibitory effect. The FA is an intermediate polyphenolic compound of curcumin, a very well-known natural antioxidant and a biologically active compound. The advantage of FA over curcumin is its relative higher solubility compared to curcumin. Like

curcumin, FA also shows anti-amyloidogenic activities. The difference in the aggregation inhibition efficiency of FA and other small molecules like curcumin may be due to a different mode of binding with the corresponding proteins.<sup>71–73</sup> The literature survey indicated that FA is effective to inhibit aggregation of a small  $\beta$ -sheeted protein A $\beta$  (containing 42 amino acid residues) in 1:4 (A $\beta$ :FA) molar ratio.<sup>73</sup> Our aim for this study was to check its inhibitory effect on a  $\beta$ -sheet predominant large protein, like  $\beta$ -Ig (containing 162 amino acid residues), and we observed satisfactory results. However, in comparison with other A $\beta$  aggregation inhibitors, FA showed better result and also proved its efficacy as a potent inhibitor of aggregation of a large protein like  $\beta$ -Ig which can be shown in the Table 2.

### 3.11 Docking results

Docking study predicts position, microenvironment and non-covalent forces involved in a small molecule-protein binding.<sup>74,75</sup> Here, we can speculate these features for FA- $\beta$ -Ig interactions with the help of docking. The result allows the perception that the FA molecule is docked on the  $\beta$ -Ig surface near N-terminal residue (Figure 7a). Ionic interactions found

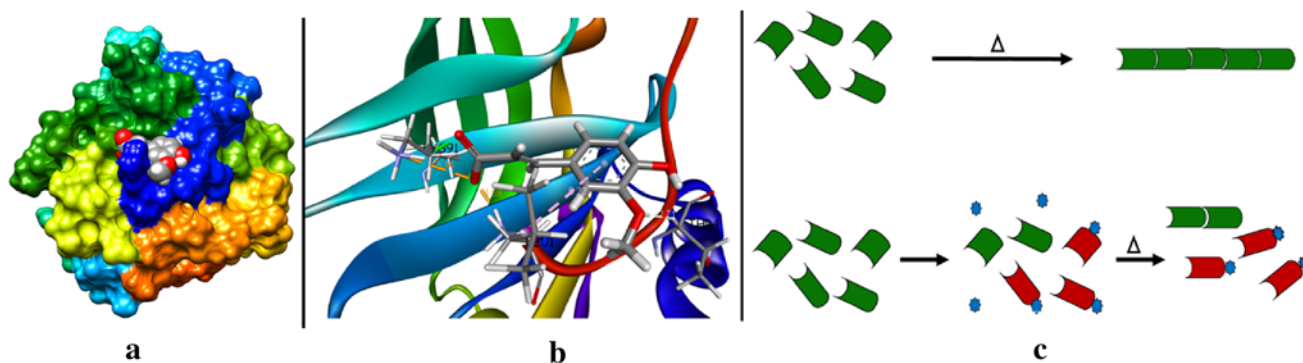


**Figure 7.** Docking pose of (a) bind site of FA on  $\beta$ -Ig surface, (b) binding modes. (c) Probable mechanism of inhibition of aggregation.

between N-terminal  $-NH_3$  of Lue1 and Lys-91 amino acid with carboxylic group of FA, separately. The  $-NH_3$  group of Lys-91 also forms a hydrogen bonding with carboxylic group of FA. One  $\pi$ -alkyl and oxygen lone pair-HC interactions also found between FA and Lue1 and Thr4 residue, respectively (Figure 7b). To understand the probable protein aggregation inhibition mechanism of FA, the docking study is of immense importance. The protein molecules have a different conformation, but some of them can induce the aggregation process through joining protein with similar conformation, one by one. This type of aggregations leads to fibril formations. Here, the FA molecule forms ionic and hydrogen bonding interactions (strongest among all non-covalent interactions) which can stabilize the conformation of protein where it binds. Therefore, such binding can lock a protein conformation and provide less scope to achieve the protein conformer responsible for aggregation. It may be a probable mechanism of inhibition to form large  $\beta$ -lg aggregates through FA- $\beta$ -lg interactions (Figure 7c).

#### 4. Conclusion

In this study, we examined the inhibitory effect of a phenolic acid, FA, on heat-induced fibrillation of bovine  $\beta$ -lactoglobulin by utilizing different biophysical methods. It has been observed that FA can strongly inhibit the thermal  $\beta$ -lactoglobulin fibrillation in a 10-fold molar excess over protein concentration. The inhibitory potency of FA *in vitro* fibril formation was concentration-dependent. At higher concentrations, FA prevents the conformation alteration of the protein from  $\beta$ -sheet  $\rightarrow$   $\alpha$ -helical structure. All spectroscopic result confirmed that FA protected the native form of  $\beta$ -lg, thereby inhibited the conformational alteration required for its amyloid fibril formation under thermal condition. Moreover, results from molecular docking study suggested that phenyl, hydroxyl and carboxylic groups in FA contribute towards its inhibitory action against  $\beta$ -lg amyloid fibrillation. Thus, from our findings, it may be reasonable to consider that FA could prevent the progress of amyloid fibril formation.

#### Acknowledgements

This work was financially supported by University Grant Commission (UGC)-CAS-II and DST-PURSE-II Program of Jadavpur University, Kolkata. Sampa Pal is receiver of UGC-BSR Research Fellowship in Science and the Meritorious Student. Authors want to acknowledge Prof S.

C. Bhattacharya, Department of Chemistry, Jadavpur University, for providing the DLS instrumental facility. We acknowledge DST for funding through INSPIRE program. Authors wish to thank Dr. Dipankar Mandal, Department of Physics, Jadavpur University, for providing the FTIR instrumental facility.

#### References

- Baskakov I V, Legname G, Prusiner S B and Cohen F E 2001 Folding of prion protein to its native alpha-helical conformation is under kinetic control *J. Biol. Chem.* **276** 19687
- Dobson C M 2003 Protein folding and misfolding *Nature* **426** 884
- Selkoe D J 2003 Folding proteins in fatal ways *Nature* **426** 900
- Temussi P A, Masino L and Pastore A 2003 From Alzheimer to Huntington: why is a structural understanding so difficult? *EMBO J.* **22** 355
- Westermarck P, Benson M D, Buxbaum J N, Cohen A S, Frangione B, Ikeda S, Masters C L, Merlini G, Saraiva M J and Sipe J D 2002 Amyloid fibril protein nomenclature—2002 *Amyloid* **9** 197
- Zerovnik E 2002 Amyloid-fibril formation *Eur. J. Biochem.* **269** 3362
- Sunde M and Blake C C F 1998 From the globular to the fibrous state: protein structure and structural conversion in amyloid formation *Q. Rev. Biophys.* **31** 1
- Arora A, Ha C and Park C B 2004 Insulin amyloid fibrillation at above 100 degrees c: new insights into protein folding under extreme temperatures *Protein Sci.* **13** 2429
- Dirix C, Meersman F, MacPhee C E, Dobson C M and K. Heremans 2005 High hydrostatic pressure dissociates early aggregates of TTR105-115, but not the mature amyloid fibrils. *J. Mol. Biol.* **347** 903
- Nordstedt C, Näslund J, Tjernberg L O, Karlström A R, Thyberg J, Terenius L 1994 The Alzheimer a beta peptide develops protease resistance in association with its polymerization into fibrils *J. Biol. Chem.* **269** 30773
- Surmacz-Chwedoruk W, Nieznańska H, Wójcik S and Dzwolak W 2012 Cross-seeding of fibrils from two types of insulin induces new amyloid strains *Biochemistry* **51** 9460
- Jha S, Sellin D, Seidel R and Winter R 2009 Amyloidogenic propensities and conformational properties of proiapp and iapp in the presence of lipid bilayer membranes *J. Mol. Biol.* **389** 907
- Klabunde T, Petrassi H M, Oza V B, Raman P, Kelly W J and Sacchettini J C 2000 Rational design of potent human transthyretin amyloid disease inhibitors *Nat. Struct. Biol.* **7** 312
- Mazaheri M, Moosavi-Movahedi A A, Saboury A A, Khodaghali F, Shaerzadeh F and Sheibani N 2015 Curcumin protects  $\beta$ -lactoglobulin fibril formation and fibril-induced neurotoxicity in pc12 cells *PLoS One* **10** e0133206. <https://doi.org/10.1371/journal.pone.0133206>
- Rivers R C, Kumita J R, Tartaglia G G, Dedmon M M, Pawar A, Vendruscolo M, Dobson C M and Christodoulou J 2008 Molecular determinants of the

- aggregation behavior of alpha- and beta-synuclein *Protein Sci.* **17** 887
16. Taylor J P, Hardy J and Fischbeck K H 2002 Toxic proteins in neurodegenerative disease *Science* **296** 1991
  17. Bemporad F, Calloni G, Campioni S, Plakoutsi G, Taddei N and Chiti F 2006 Sequence and structural determinants of amyloid fibril formation *Acc. Chem. Res.* **39** 620
  18. Fandrich M, Fletcher M A and Dobson C M 2001 Amyloid fibrils from muscle myoglobin *Nature* **410** 165
  19. Nielsen L, Khurana R, Coats A, Frokjaer S, Brange J V N, Uversky A and Fink L 2001 Effect of environmental factors on the kinetics of insulin fibril formation: elucidation of the molecular mechanism *Biochemistry* **40** 6036
  20. Yang M and Teplow D B 2008 Amyloid beta-protein monomer folding: free-energy surfaces reveal alloform-specific differences *J. Mol. Biol.* **384** 450
  21. Maity S, Sardar S, Pal S, Parvej H, Chakraborty J and Halder U C 2016 Multispectroscopic analysis and molecular modeling to investigate the binding of beta lactoglobulin with curcumin derivatives *RSC Adv.* **6** 74409
  22. Pal S, Maity S, Sardar S, Chakraborty J and Halder U C 2016 Insight into the co-solvent induced conformational changes and aggregation of bovine  $\beta$ -lactoglobulin *Int. J. Biol. Macromol.* **84** 121
  23. Schmit J D, Ghosh K and Dill K 2011 What drives amyloid molecules to assemble into oligomers and fibrils? *Biophys. J.* **100** 450
  24. Sardar S, Anas M, Maity S, Pal S, Parvej H, Begum S, Dalui R, Sepay N and Halder U C 2019 Silver nanoparticle modulates the aggregation of beta-lactoglobulin and induces to form rod-like aggregates *Int. J. Biol. Macromol.* **125** 596
  25. Alam P, Beg A Z, Siddiqi M K, Chaturvedi S K, Rajpoot R K, Ajmal M R, Zaman M, Abdelhameed A S and Khan R H 2017 Ascorbic acid inhibits human insulin aggregation and protects against amyloid induced cytotoxicity *Arch. Biochem. Biophys.* **621** 54
  26. Ono K, Hamaguchi T, Naiki H and Yamada M 2006 Anti-amyloidogenic effects of antioxidants: implications for the prevention and therapeutics of Alzheimer's disease *Biochim. Biophys. Acta Mol. Basis Dis.* **1762** 575
  27. Roth A, Schaffner W and Hertel C 1999 Phytoestrogen Kaempferol (3,4',5,7-tetrahydroxyflavone) protects PC12 and T47D cells from beta-amyloid-induced toxicity *J. Neurosci. Res.* **57** 399
  28. Alam P, Siddiqi M K, Chaturvedi S K, Zaman M and Khan R H 2017 Vitamin B12 offers neuronal cell protection by inhibiting A $\beta$ -42 amyloid fibrillation *Int. J. Biol. Macromol.* **99** 477
  29. Ono K., Hasegawa K, Naiki H and Yamada M 2004 Curcumin has potent anti-amyloidogenic effects for alzheimer's beta-amyloid fibrils in vitro *J. Neurosci. Res.* **75** 742
  30. Borana M S, Mishra P, Pissurlenkar R R, Hosur R V and Ahmad B 2014 Curcumin and kaempferol prevent lysozyme fibril formation by modulating aggregation kinetic parameters *Biochim. Biophys. Acta, Proteins Proteom.* **1844** 670
  31. Abbas S and Wink M 2010 Epigallocatechin gallate inhibits beta amyloid oligomerization in *Caenorhabditis elegans* and affects the *daf-2*/insulin-like signaling pathway *Phytomedicine* **17** 902
  32. Ehrnhoefer D E, Bieschke J, Boeddrich A, Herbst M, Masino L, Lurz R, Engemann S, Pastore A and Wanker E E 2008 EGCG redirects amyloidogenic polypeptides into unstructured, off-pathway oligomers *Nat. Struct. Mol. Biol.* **15** 558
  33. Cai Y, Baer-Dubowska W, Ashwood-Smith M J, Ceska O, Tachibana S and Di-Giovanni J 1996 Mechanism-based inactivation of hepatic ethoxyresorufin o-dealkylation activity by naturally occurring coumarins *Chem. Res. Toxicol.* **9** 729
  34. Cui L, Zhang Y, Cao H, Wang Y, Teng T, Ma G, Li Y, Li K and Zhang Y 2013 Ferulic acid inhibits the transition of amyloid- $\beta$ 42 monomers to oligomers but accelerates the transition from oligomers to fibrils *J. Alzheimer's Dis.* **37** 19
  35. Bonina F P, Leotta C, Scalia G, Puglia C, Trombetta D, Tringali G, Roccazzello A M, Rapisarda P and Saija A 2002 Evaluation of oxidative stress in diabetic patients after supplementation with a standardised red orange extract *Diabetes, Nutr. Metab.* **15** 14
  36. Graf E 1992 Antioxidant potential of ferulic acid *Free Radic. Biol. Med.* **13** 435
  37. Sgarbossa A, Giacomazza D and di Carlo M 2015 Ferulic acid: a hope for alzheimer's disease therapy from plants *Nutrients* **7** 5764
  38. Shoval H, Weiner L, Gazit E, Levy M, Pinchuk I and Lichtenberg D 2008 Polyphenol-induced dissociation of various amyloid fibrils results in a methionine-independent formation of ROS *Biochim. Biophys. Acta Proteins Proteom.* **1784** 1570
  39. Ono K, Hirohata M and Yamada M 2005 Ferulic acid destabilizes preformed beta-amyloid fibrils in vitro *Biochem. Biophys. Res. Commun.* **336** 444
  40. Alam M A, Sernia C and Brown L 2013 Ferulic acid improves cardiovascular and kidney structure and function in hypertensive rats *J. Cardiovasc. Pharmacol.* **61** 240
  41. Sompong W, Meeprom A, Cheng H and Adisakwattana S 2013 A comparative study of ferulic acid on different monosaccharide-mediated protein glycation and oxidative damage in bovine serum albumin *Molecules* **18** 13886
  42. Sultana R 2012 Ferulic acid ethyl ester as a potential therapy in neurodegenerative disorders *Biochim. Biophys. Acta Mol. Basis Dis.* **1822** 748
  43. Taniguchi H, Hosoda A, Tsuno T, Maruta Y and Nomura E 1999 Preparation of ferulic acid and its application for the synthesis of cancer chemopreventive agents *Anticancer Res.* **19** 3757
  44. Brownlow S, Cabral J H M, Cooper R, Flower D R, Yewdall S J, North A C T and Sawyer L 1997 Bovine  $\beta$ -lactoglobulin at 1.8 Å resolution—still an enigmatic lipocalin *Structure* **5** 481
  45. Fox P F, Sweeney M and Paul L H 2003 *Advanced dairy chemistry: volume 1: proteins, parts A & B*, 3rd edn. Kluwer Academic/Plenum Publishers, New York
  46. Burova T V, Choiset Y, Tran V and Haertlé T 1998 Role of free Cys121 in stabilization of bovine beta-lactoglobulin B *Protein Eng.* **11** 1065

47. Carrotta R, Arleth L, Pedersen J S and Bauer R 2003 Small-angle X-ray scattering studies of metastable intermediates of  $\beta$ -lactoglobulin isolated after heat-induced aggregation *Biopolymers* **70** 377
48. Fitzsimons S M, Mulvihill D M and Morris E R 2007 Denaturation and aggregation processes in thermal gelation of whey proteins resolved by differential scanning calorimetry *Food Hydrocoll.* **21** 638
49. Navarra G, Leone M and Militello V 2007 Thermal aggregation of  $\beta$ -lactoglobulin in presence of metal ions *Biophys. Chem.* **131** 52
50. Arnaudov L N, de Vries R, Ippel H and van Mierlo C P M 2003 Multiple steps during the formation of  $\beta$ -lactoglobulin fibrils *Biomacromolecules* **4** 1614
51. Relkin P 1998 Reversibility of heat-induced conformational changes and surface exposed hydrophobic clusters of beta-lactoglobulin: their role in heat-induced sol-gel state transition *Int. J. Biol. Macromol.* **22** 59
52. Chakraborty J, Das N, Das K P and Halder U C 2009 Loss of structural integrity and hydrophobic ligand binding capacity of acetylated and succinylated bovine  $\beta$ -lactoglobulin *Int. Dairy J.* **19** 43
53. Semisotnov G V, Radionava N A, Razgulyaev O I, Uversky V N, Gripas A F and Gilmanshin R I 1991 Study of the "Molten Globule" intermediate state in protein folding by a hydrophobic fluorescent probe *Biopolymer* **31** 119
54. Nilsson M R 2004 Techniques to study amyloid fibril formation in vitro *Methods* **34** 151
55. Hudson S A, Ecroyd H, Kee T W and Carver J A 2009 The thioflavin T fluorescence assay for amyloid fibril detection can be biased by the presence of exogenous compounds *FEBS J.* **276** 5960
56. Yu W W, Chang E, Falkner J C, Zhang J, Al-Somali A M, Sayes C M, Johns J, Drezek R and Colvin V L 2007 Forming biocompatible and nonaggregated nanocrystals in water using amphiphilic polymers *J. Am. Chem. Soc.* **129** 2871
57. Bannerjee V and Das K P 2012 Modulation of pathway of insulin fibrillation by a small molecule helix inducer 2,2,2-trifluoroethanol *Colloids Surf. B Biointerfaces* **92** 142
58. Busti P, Gatti C A and Delorenzi N J 1998 Some aspects of beta-lactoglobulin structural properties in solution studied by fluorescence quenching *Int. J. Biol. Macromol.* **23** 143
59. (a) Gosal W S, Clark A H and Ross-Murphy S B 2004 Fibrillar beta-lactoglobulin gels: part 1. fibril formation and structure *Biomacromolecules* **5** 2408; (b) Kayser J J, Arnold P, Steffen-Heins A, Schwarz K and Keppler J K 2020 Functional ethanol-induced fibrils: influence of solvents and temperature on amyloid-like aggregation of beta-lactoglobulin *J. Food Eng.* **270** 109764; (c) Maity S, Sardar S, Pal S, Parvej H, Chakraborty J and Halder U C 2016 New insight into the alcohol induced conformational change and aggregation of the alkaline unfolded state of bovine  $\beta$ -lactoglobulin *RSC Adv.* **6** 74409
60. Matulis D, Baumann C G, Bloomfield V A and Lorvine R E 1999 1-Anilino-8-naphthalene sulfonate as a protein conformational tightening agent *Biopolymers* **49** 451
61. Collini M, D'Alfano L, Molinari H, Ragona L, Catalano M and Baldini G 2003 Competitive binding of fatty acids and the fluorescent probe 1-8-anilino-naphthalene sulfonate to bovine beta-lactoglobulin *Protein Sci.* **12** 1596
62. Sardar S, Pal S, Maity S, Chakraborty J and Halder U C 2014 Amyloid fibril formation by  $\beta$ -lactoglobulin is inhibited by gold nanoparticles *Int. J. Biol. Macromol.* **69** 137
63. Biancalana M and Koide S 2010 Molecular mechanism of thioflavin-T binding to amyloid fibrils *Biochim. Biophys. Acta Proteins Proteom.* **1804** 1405
64. Khurana R, Coleman C, Ionescu-Zanetti C, Carter S A, Krishna V, Grover R K, Roy R and Singh S 2005 Mechanism of thioflavin T binding to amyloid fibrils *J. Struct. Biol.* **151** 229
65. Jayamani J, Shanmugam G and Singam E R A 2014 Inhibition of insulin amyloid fibril formation by ferulic acid, a natural compound found in many vegetables and fruits *RSC Adv.* **4** 62326
66. Bramanti E, Fulgentini L, Bizzarri R, Lenci F and Sgarbossa A 2013  $\beta$ -Amyloid amorphous aggregates induced by the small natural molecule ferulic acid *J. Phys. Chem. B* **117** 13816
67. Kuznetsova I M, Sulatskaya A I, Uversky V N and Turoverov K K 2012 A new trend in the experimental methodology for the analysis of the thioflavin T binding to amyloid fibrils *Mol. Neurobiol.* **45** 488
68. Khan J M, Qadeer A, Chaturvedi S K, Ahmad E, Abdul Rehman S A, Gourinath S and Khan R H 2012 SDS can be utilized as an amyloid inducer: a case study on diverse proteins *PLoS One* **7** e29694.
69. Bahttacharjee C, Saha S, Biswas A, Kundu M, Ghosh L and Das K P 2005 Structural changes of  $\beta$ -lactoglobulin during thermal unfolding and refolding—an FT-IR and circular dichroism study *Protein J.* **24** 27
70. Pal S, Maity S, Sardar S, Parvej H, Das N, Chakraborty J and Halder U C 2016 Curcumin inhibits the Al(iii) and Zn(ii) induced amyloid fibrillation of  $\beta$ -lactoglobulin in vitro *RSC Adv.* **6** 111299
71. Maity S, Pal S, Sardar S, Sepay N, Parvej H, Begum S, Dalui R, Das N, Pradhan A and Halder U C 2018 Inhibition of amyloid fibril formation of  $\beta$ -lactoglobulin by natural and synthetic curcuminoids *New J. Chem.* **42** 19260
72. Necula M, Kayed R, Milton S and Glabe C G 2007 Small molecule inhibitors of aggregation indicate that amyloid beta oligomerization and fibrillization pathways are independent and distinct *J. Biol. Chem.* **282** 10311
73. Bramanti E, Fulgentini L, Bizzarri R, Lenci F and Sgarbossa A 2013  $\beta$ -Amyloid amorphous aggregates induced by the small natural molecule ferulic acid *J. Phys. Chem. B* **117** 13816
74. Sepay N, Mallik S, Guha C and Mallik A K 2016 An efficient synthesis of 1,3-dimethyl-5-(2-phenyl-4H-chromen-4-ylidene) pyrimidine-2,4,6(1H,3H,5H)-triones and investigation of their interactions with  $\beta$ -lactoglobulin *RSC Adv.* **6** 96016
75. Sepay N, Guha C, Maity S and Mallik A K 2017 Synthesis of 6,12-methanobenzo[d]pyrano[3,4-g][1,3]-dioxocin-1(12h)-ones and study of their interaction with DNA and  $\beta$ -lactoglobulin *Eur. J. Org. Chem.* **2017** 6013